000 Solid tumors versus mixed tumors with a ground-glass opacity component in patients with clinical stage IA lung adenocarcinoma: Prognostic comparison using high-resolution computed tomography findings

Yasuhiro Tsutani, MD, PhD, Yoshihiro Miyata, MD, PhD, Takeharu Yamanaka, PhD, Haruhiko Nakayama, MD, PhD, Sakae Okumura, MD, PhD, Shuji Adachi, MD, PhD, Masahiro Yoshimura, MD, PhD, and Morihito Okada, MD, PhD, Hiroshima, Kashiwa, Yokohama, Tokyo, and Akashi, Japan

In patients with clinical stage IA lung adenocarcinomas, solid tumors exhibit more malignant behavior compared with mixed tumors having ground-glass opacity components, even after solid component size is matched on high-resolution computed tomography. However, malignant behavior can be elucidated using maximum standardized uptake values on F-18-fluorodeoxyglucose positron emission tomography/computed tomography.

Cancer Science
The official journal of the Japanese Cancer Association JCA

Antitumor activity of human γδ T cells transducted with CD8 and with T-cell receptors of tumor-specific cytotoxic T lymphocytes

Takeshi Hanagiri,[1] Yoshiki Shigematsu, Koji Kuroda, Tetsuro Baba, Hironobu Shiota, Yoshinobu Ichiki, Yoshika Nagata, Manabu Yasuda, Tomoko So, Mitsuhiro Takenoyama and Fumihiro Tanaka

Second Department of Surgery, School of Medicine, University of Occupational and Environmental Health, Kitakyushu, Japan

(Received March 1, 2012/Revised May 1, 2012/Accepted May 8, 2012/Accepted manuscript online May 24, 2012/Article first published online July 6, 2012)

The difficulty in the induction and preparation of a large number of autologous tumor-specific cytotoxic T lymphocytes (CTL) from individual patients is one of major problems in their application to adoptive immunotherapy. The present study tried to establish the useful antitumor effectors by using γδ T cells through tumor-specific TCRαβ genes transduction, and evaluated the efficacy of their adoptive transfer in a non-obese diabetic/severe combined immunodeficiency (NOD/SCID) mice model. The TCRαβ gene was cloned from the HLA-B15-restricted CTL clone specific of the Kita-Kyushu Lung Cancer antigen-1 (KK-LC-1). The cloned TCRαβ as well as the CD8 gene were transduced into γδ T cells induced from peripheral blood lymphocytes (PBL). Cytotoxic T lymphocyte activity was examined using a standard 4 h ^{51}Cr release assay. Mice with a xenotransplanted tumor were treated with an injection of effector cells. Successful transduction of TCRαβ was confirmed by the staining of KK-LC-1-specific tetramers. The γδ T cells transduced with TCRαβ and CD8 showed CTL activity against the KK-LC-1-positive lung cancer cell line in a HLA B15-restricted manner. Adoptive transfer of the effector cells in a mice model resulted in marked growth suppression of KK-LC-1- and HLA-B15-positive xenotransplanted tumors. Co-transducing TCRαβ and CD8 into γδ T cells yielded the same antigen-specific activity as an original CTL *in vitro* and *in vivo*. The TCRαβ gene transduction into γδ T cells is a promising strategy for developing new adoptive immunotherapy. (*Cancer Sci* 2012; 103: 1414–1419)

Lung cancer is the most common malignant neoplasm and the leading cause of cancer mortality in industrialized countries.[1] In spite of advances in diagnostic and therapeutic approaches against lung cancer, there has been limited improvement in treatment outcome. Recent clinical studies on immunotherapy indicate favorable therapeutic effects, and might become one of the alternative treatment approaches for lung cancer.[2–4] The adoptive transfer of tumor-infiltrating lymphocytes after the administration of lymphodepleting preparative regimen mediates objective cancer regression in 50% of patients with metastatic melanoma.[5] However, the difficulty in the induction and expansion of a large number of autologous tumor-specific cytotoxic T lymphocytes (CTL) from individual patients is one of the major problems in their application to adoptive immunotherapy. To overcome this drawback, T-cell receptors (TCR) can be harnessed with antitumor specificities via molecular techniques. T-cell receptors with known antitumor reactivity can be genetically introduced into primary human T lymphocytes and provide effective tools for immunogenic therapy of tumors.[6]

In contrast, human γδ T cells can recognize and respond to a wide variety of stress-induced antigens, thereby developing innate broad antitumor and anti-infective activity.[7] These cells recognize antigens in a HLA complex-independent manner and develop strong cytolytic and Th1-like effector functions.[7] Furthermore, human γδ T cells can be activated by phospho-antigens and aminobisphosphonates. Aminobisphosphonates also facilitate large-scale *ex vivo* expansion of functional γδ T cells from the peripheral blood of cancer patients.[8] Although the antitumor effect is not antigen-specific cytotoxicity, γδ T cells are attractive candidate effector cells for cancer immunotherapy.

Kita-Kyushu Lung Cancer antigen-1 (KK-LC-1) is a recently identified cancer/testis (CT) antigen from lung adenocarcinoma.[9] KK-LC-1 is a cancer/testis antigen because it is not expressed in normal tissues except for the testis, and is located on the X chromosome (Xq 22). A 9-mer peptide (KK-LC-1_{76-84}; RQKRILVNL) is recognized by CTL in a HLA B15-restricted manner. The present study tried to establish a useful antitumor effector by using γδ T cells through tumor-specific TCR αβ genes transduction derived from a KK-LC-1-specific CTL clone, and evaluated the efficacy of their adoptive transfer in a severe combined immunodeficiency (SCID) mice model.

Materials and Methods

The study protocol was approved by the Human and Animal Ethics Review Committee of University of Occupational and Environmental Health and a signed consent form was obtained from each patient before taking the tissue samples used in the present study.

Culture medium. The culture medium for the cell lines was RPMI 1640 (GIBCO-BRL, Grand Island, NY, USA) supplemented with 10% heat-inactivated fetal calf serum (FCS; Equitech-Bio, Ingram, TX, USA), 10 mM HEPES, 100 U/mL of penicillin G and 100 mg/mL of streptomycin sulfate. The culture medium for γδ T cells and γδ T cells transduced with TCRαβ and CD8 genes was AlyS203-700 (Cell Science and Technology Institute, Sendai, Japan) supplemented with 10% heat-inactivated FCS. The γδ T cells were expanded with 1 μM Zoledronate (Novartis, Basel, Switzerland) followed by the addition of 100 units/mL interleukin-2 (IL-2) (Fig. 1).

Cell lines. F1121L, A110L and B901L lung adenocarcinoma cell lines were established from surgical specimens, which had the genotype of HLA-A*2402/0201, B*4006/1507, Cw*0303/0801, HLA-A*2402/, B*5201/, Cw*1201/, and HLA-A*0206/2601, B*3901/4006, Cw*0702/0801, respectively. The three lung adenocarcinoma cell lines showed a positive expression for KK-LC-1. The method used to establish the lung cancer cell line has been described previously.[10] F1121 Epstein–Barr virus-transformed B cells (F1121 EBV-B) were derived from

[1]To whom correspondence should be addressed.
E-mail: hanagiri@med.uoeh-u.ac.jp

doi: 10.1111/j.1349-7006.2012.02337.x

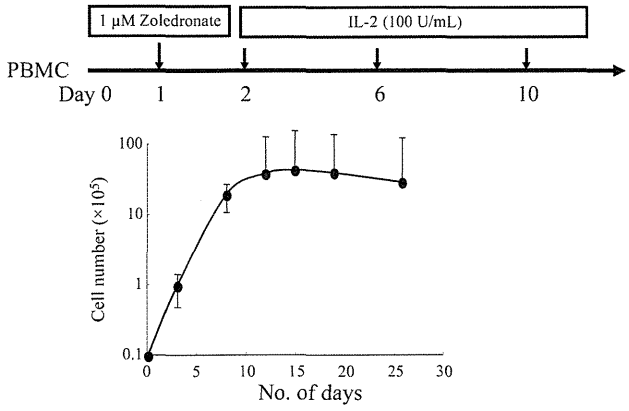

Fig. 1. Proliferation of γδ T cells in the presence of zoledronate and interleukin-2 (IL-2). The γδ T cells expanded 400-fold 2 weeks after stimulation with zoledronate in the presence of IL-2 100 U/mL.

peripheral blood lymphocytes (PBL) of F1121 treated with 1 μg/mL cyclosporine A (Sandoz, Basel, Switzerland) and 20% of the supernatant of the Epstein–Barr virus-transformed marmoset monkey lymphocyte B95-8. K562 is an erythroleukemia cell line that is sensitive to natural killer cell cytotoxicity. Tumor necrosis factor (TNF)-sensitive WEHI 164c13 cells were kindly donated by Dr Coulie PG (Cellular Genetics Unit, Universite Catholic de Louvaine, Brussels, Belgium). WEHI-164c13 cells were maintained in culture medium with 5% FCS.

TCRαβ gene cloning from KK-LC-1$_{76-84}$-specific CTL clone. The TCRαβ gene was cloned from the HLA-B15-restricted CTL clone specific for KK-LC-1 (cancer/testis antigen), which was identified from a patient with lung adenocarcinoma.[9] The cloned TCRα and TCRβ were then joined by a picornavirus-like 2A 'self-cleaving' peptide by overlapping PCR. The short 18 amino acid 2A sequence that separates the TCR α and TCR β results in equimolar expression of the TCRαand TCRβvia a 'ribosomal skip' mechanism.[11] The TCR α and TCR β combined with the 2A sequence were cloned into a pMX retroviral vector. The pMX vector harbors a 5′ long terminal repeat (LTR) and the extended packaging signal derived from a MFG vector followed by a multi-cloning site suitable for cDNA construction and 3′ LTR of Moloney murine leukemia virus. The resulting vector pMX in combination with Plat-A cells (Cell Biolabs Inc., San Diego, CA, USA) produces an average of 1×10^7 IU/mL of virus.[12] pMX-vector had a conjugated puromycine-resistant gene for the selection of the transductant.

TCRαβ gene transduction using retroviral vector. An infectious, replication-incompetent retrovirus was produced using the pMX retroviral vector system with Plat-A cells and the Lipofectamine 2000 reagent (Invitrogen, Carlsbad, CA, USA). Briefly, Plat-A cells were transfected with the TCR containing plasmid. After 1 day culture from the transfection, supernatant of Plat-A cells was harvested, filtered using a 0.22 mm sterile filter and concentrated by centrifugation at 5800*g* overnight. Concentrated supernatant containing retrovirus was used for the gene transduction. The cloned TCR αβ as well as the CD8 gene (provided by Takara Bio Inc., Otsu, Japan) were transduced into γδ T cells induced from PBL by using a retroviral vector in recombinant human fibronectin fragment CH-296 (Retronectin, Takara Bio)-coated six-well plates (Nunc, Roskilde, Denmark). The transduction was repeated the following day. Cytotoxic T lymphocyte activity was examined using a cytotoxicity assay and a cytokine production assay.

KK-LC-1/HLA-B15 tetramer staining. The transduction of TCRαβ was confirmed by the staining of KK-LC-1-specific tetramers. KK-LC-1-specific tetramers (T-Select MHC Tetramer) were purchased from Medical & Biological Laboratories Co., Ltd (Nagoya, Japan). TCRαβ-transduced γδ T cells were washed and resuspended in PBS with 1% human AB serum, and incubated for 30 min at 37°C with the KK-LC-1$_{76-84}$/HLA-B15 tetramer (20 nM each) coupled with phycoerythrin. The cells were washed, fixed with 0.5% formaldehyde and analyzed on a FACS Calibur flow cytometer (BD Biosciences, San Jose, CA, USA) using the FlowJo software package (Tree Star Inc., OR, USA).

Monoclonal antibody (mAb) for cytotoxicity assay and cytokine production. Hybridomas (HB-145, HB-95) were purchased from the American Type Culture Collection (ATCC, Rockville, MD, USA). C7709.A2.6 (anti-HLA-A24) and B1.23.2 (anti-HLA-B, C) were kindly donated by Dr Coulie PG. The culture supernatants of ATCC HB–145 (IVA12; anti-HLA-DR, DP, DQ) and HB-95 (W6/32; anti-HLA-A, B, C) were used for analyzing the HLA restriction of CTL and antitumor effectors. The anti-NKG2D antibody was purchased from BD Biosciences.

Cytotoxicity assay and cytokine production of CTL. The cytotoxicity of CTL was assessed using a standard 4 h ^{51}Cr release assay as described previously.[13] The TNF production of CTL was measured using a WEHI assay using TNF-sensitive WEHI cells.[13] Briefly, CTL clone L7/8 (6×10^4/mL) TCR-transduced γδ T cells was incubated with tumor cells (6×10^5/mL) in culture medium with 10% FCS overnight and the amount of TNF in the culture supernatant was measured in a triplicate assay by evaluation of the cytotoxic effect on WEHI-164c13 cells in a MTT colorimetric assay. Supernatants were also collected to measure interferon–γ (IFN-γ) production in a triplicate assay using an IFN-γ ELISA test kit (Life technologies, Inc., Gaithersburg, MD, USA) according to the manufacturer's instructions. In the blocking assay using mAb, a¼-diluted culture supernatant of hybridomas such as HB-95, C7709.A2.6, B1.23.2 and HB-145 was used for the antibody inhibition assay.

Lung adenocarcinoma xenograft model. The γδ T cells were expanded from peripheral blood mononuclear cells (PBMC) of patients with adenocarcinoma with 100 units/mL rIL-2 after stimulation with zoledronate. The number of γδ T cells was calculated with a flow cytometer by using anti-TCR γδ ((BD Biosciences). The activated γδ T cells were transduced with TCR αβ gene derived from a KK-LC-1-specific CTL clone; the antitumor effect was assessed in a lung adenocarcinoma (B901L) xenotransplanted non-obese diabetic/severe combined immunodeficiency (NOD/SCID) mouse model. The parental B901L cell line expresses KK-LC-1 but does not possess the HLA-B15 molecule. B901L-parental and HLA-B15 transduced B901L were inoculated subcutaneously with 1×10^6 cells in the lateral flank of a NOD/SCID mouse at day 0. TCRαβ and CD8 transduced γδ T cells were injected via the tail vein of immunodeficient mice (NOD/SCID mice) weekly or twice weekly. Vehicle (PBS) was injected intravenously in the same manner. The effects of treatment were evaluated by measuring tumor size. The volume of the tumor was calculated using the formula: $v = 0.4 \times a \times b^2$, where a is the maximum diameter of the tumor, and b is the diameter at a right angle to a.

Results

***In vitro* expansion of γδ T cells.** The γδ T cells could easily be expanded with 1 μM of zoledronate in the presence of IL-2 100 U/mL. Flow cytometry of the cultured cells revealed that the population of γδ T cells in the PBMC was 2–3% initially, and increased more than 95% at day 14. The number of γδ T cells could be expanded approximately 400-fold during the 2 weeks after stimulation with zoledronate (Fig. 1). The

growth curves of the γδ T cells are shown as mean ± standard deviation on the basis of three independent experiments.

Transduction of the TCRαβ gene of tumor-specific CTL. The TCRαβ gene was cloned from the HLA-B15-restricted CTL clone specific for KK-LC-1 (cancer/testis antigen), which was established from a patient with lung adenocarcinoma. The original CTL clone specific for KK-LC-1 showed positive staining with the KK-LC-$1_{76\text{-}84}$/HLA-B15 tetramer. The γδ T cells were negative for the KK-LC-$1_{76\text{-}84}$/HLA-B15 tetramer. The cloned TCRαβ and CD8 genes were co-transduced into the γδ T cells. After transduction of the TCRαβ gene, expression of the TCR specific for KK-LC-1 was confirmed by flow cytometry staining with the KK-LC-$1_{76\text{-}84}$/HLA-B15 tetramer (Fig. 2). The tetramer staining was positive more than 80% after puromycine selection. The data of flow cytometry shown are representative of at least three independent experiments. The effector cells were used for further experiments when the staining for the KK-LC-$1_{76\text{-}84}$/HLA-B15 tetramer was confirmed to be more than 80% positive.

Cytotoxic T lymphocyte activity of γδ T cells co-transducted with the TCR gene and the CD8 gene. The CTL activity against the KK-LC-1 epitope was examined using a cytotoxicity assay and cytokine production assay. The γδ T cells indicated strong natural killer (NK) activity and non-specific cytotoxicity against the allogeneic lung cancer cell line (Fig. 3A). The γδ T cells transduced with only the TCR gene showed neither CTL activity nor NK activity (Fig. 3B). NKG2D expression was examined to evaluate inhibition of the cytotoxicity of the γδ T cells after transduction with the TCR gene. The expression of NKG2D was remarkably suppressed after TCR transduction (Fig. 4). In contrast, the γδ T cells co-transfected with the TCR and CD8 genes (TCRαβ-CD8 γδ T cells) showed tumor antigen-specific cytotoxic activity that was similar to that of the original CTL clones (Fig. 3C). The NK cytotoxic activity and non-specific cytotoxicity were dramatically inhibited after TCR transduction (Fig. 3C). TCRαβ-CD8 γδ T cells produced IFN-γ in response to F1121L adenocarcinoma as well as EBV-B cells pulsed with KK-LC-1 peptide (Fig. 5). The production was blocked by anti-HLA class I antibody, anti-HLA B/C antibody and anti-CD8 antibody.

Antitumor activity of TCRαβ-CD8 γδ T cells *in vivo*. For evaluation of the effect of TCRαβ-CD8 γδ T cells *in vivo*, a HLA-B15-positive B901L (lung adenocarcinoma cell line) was established by stable transfection of the HLA-B15 gene. Parental B901L is negative for HLA-B15 but positive for KK-LC-1, and therefore the TCRαβ-CD8 γδ T cells showed cytotoxic activity against HLA-B15 transfected B901(B901L-HLA-B15), but not against parental B901L (Fig. 6). Intravenous injection of TCRαβ-CD8 γδ T cells inhibited growth of the susceptible cancer cell line of B901L-HLA-B15. B901L-parental and B901L-HLA-B15 were xenotransplanted subcutaneously in the lateral flank of a NOD/SCID mouse on day 0. The growth of the susceptible cancer cell line (B901L-HLA-B15) was inhibited significantly by weekly intravenous injection of the TCRαβ-CD8 γδ T cells (1×10^6/injection) in comparison to the control cell line (B901L; Fig. 7A). The growth rate of both cell lines was almost the same without the adoptive immunotherapy (data not shown). The growth of B901L-HLA-B15 was remarkably decreased by twice-weekly injection of the TCRαβ-CD8 γδ T cells (Fig. 7B).

Infiltration of adoptively transferred TCRαβ-CD8-γδ T cells into the tumor. The histological examination and immunohistochemical staining revealed that the CD3-positive human lymphocytes had infiltrated into the susceptible tumor (B901L-HLA-B15). The infiltration of CD3-positive human lymphocytes was observed more strongly in the B901L-HLA-B15 tumor compared with the control cell line (B901L) (Fig. 8A). The central part of the tumor (B901L-HLA-B15) exhibited necrosis. Expression of the TCR Vα13 gene of the effector cells (TCRαβ-CD8-γδ T) was identified in the central part of the tumor tissue (B901L-HLA-B15) using RT-PCR. The original CTL specific for KK-LC-1 also possessed TCR Vα13 (Fig. 8B).

Discussion

The mechanism of the antitumor immune response has been gradually elucidated based on the recent progress of molecular biological technique. However, clinical studies have not shown a satisfactory clinical response rate. The clinical outcome is still inferior to established treatment such as chemotherapy and radiotherapy.[14] Therefore, immunotherapy must overcome several problems before it becomes an established therapy for cancer patients. Adoptive immunotherapy requires the induction of tumor-reactive T lymphocytes *ex vivo* followed by expansion of these cells in order to generate sufficient numbers for infusion. Although several studies demonstrate that autologous *ex vivo*-generated antitumor CTL can be administered safely in patients with advanced solid tumors and can improve the immunological antitumor reactivity in recipients, the strategy is hampered by the difficulty of isolating and expanding a sufficient quantity of autologous tumor-reactive T cells capable of preserving the cytotoxic capacity.[15,16]

Several investigators have reported TCR transduction technology with retroviral vectors enables generation of novel effectors that demonstrate HLA-restricted, antigen-specific CTL functions.[17,18] The transduction of the TCRαβ genes facilitates production of a large number of antitumor effectors functionally similar to CTL activity in a reproducible fashion without laborious techniques.[19] However, the disadvantage of TCRαβ transfer to other αβ T cells is the possible formation

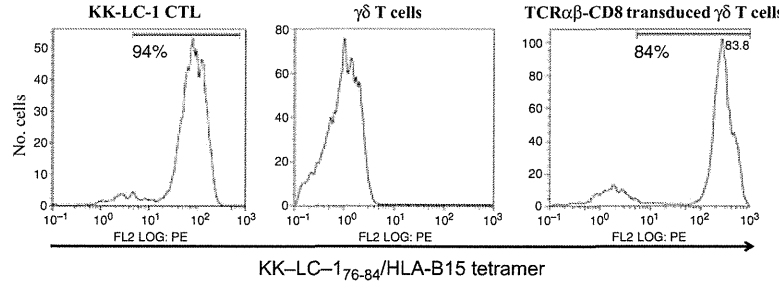

Fig. 2. KK-LC-$1_{76\text{-}84}$/HLA-B15 tetramer staining of γδ T cells transfected with TCRαβ and CD8 genes. Expression of TCRαβ was confirmed by the staining of HLA tetramers. The positive tetramer staining for specific KK-LC-$1_{76\text{-}84}$ reached more than 80% after puromycine selection.

doi: 10.1111/j.1349-7006.2012.02337.x

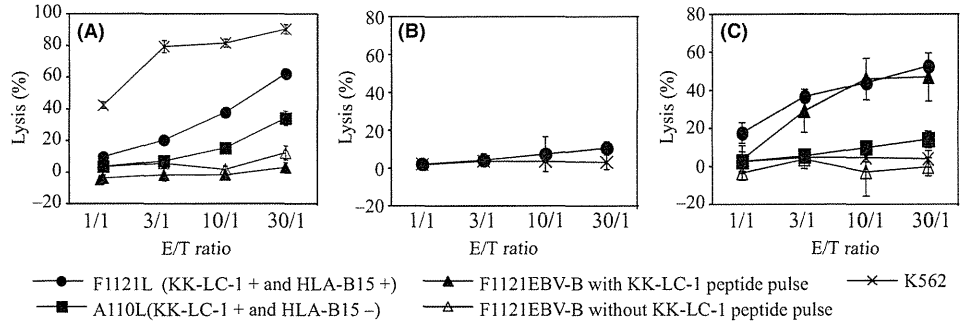

Fig. 3. Cytotoxic activity of γδ T cells transduced with TCRαβ gene derived from KK-LC-1-specific cytotoxic T lymphocytes (CTL). The γδ T cells co-transduced with TCRαβ and CD8 showed cytotoxic activity to KK-LC-1-positive tumor cells (F1121L) as well as F1121EBV-B pulsed with KK-LC-$1_{76\text{-}84}$. However the γδ T cells transduced with only *TCRαβ gene showed neither CTL activity nor natural killer (NK) activity. The effector cells were γδ T cells in (A), γδT cells transduced with only the TCR αβ gene in (B), and γδ T cells co-transduced with TCRαβ and CD8 genes in (C). E/T, effector/target.

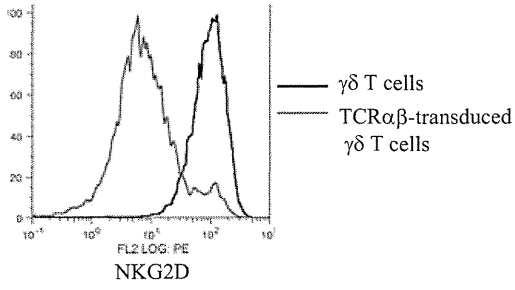

Fig. 4. Downregulation of NKG2D expression by transfection with the TCRαβ gene. NKG2D expression was measured using flow cytometry. The expression of NKG2D was remarkably suppressed after transduction of the TCR gene.

of mixed TCR heterodimers. The introduced α or β TCR could pair with the endogenous α or β TCR chains to generate unfavorable T cells with self-antigen specificity.[20,21] Okamoto *et al.*[22] reported the effect of small interfering RNA (siRNA) constructs that specifically downregulate endogenous TCR to inhibit formation of mispairing TCR heterodimers. The human lymphocytes transduced with siRNA exhibit high surface expression of the introduced tumor-specific TCR and reduced expression of endogenous TCR, and these lymphocytes transduced with tumor-specific TCR demonstrate enhanced cytotoxic activity against antigen-expressing tumor cells.

The γδ T cells account for 2–10% of T lymphocytes in human blood and also play a role in immune surveillance against microbial pathogens and cancer.[23] The γδ T cells recognize small non-peptidic phosphorylated compounds, referred to as phosphoantigens, via polymorphic γδ TCR, as well as the major histocompatibility complex class I chain-related molecules, A and B (MICA and MICB), via NKG2D receptors in a HLA-unrestricted manner.[24] The γδ T cell activation is induced by zoledronic acid through accumulation of isopentenyl diphosphate.[25] Recent studies have reported that aminobisphosphonates, currently used in cancer treatment for bone metastases, can activate γδ T cells both *in vitro* and *in vivo*.[26,27] These data suggest that γδ T cells could be an alternative population for efficient TCR transfer. Hiasa *et al.*[28] proposed γδ T cells as a target for retroviral transfer of cancer-specific TCR. They indicated that γδ T cells co-transduced with TCRαβ and CD8 alphabeta genes acquire cytotoxicity against tumor cells and produce cytokines in both αβ- and γδ-TCR- dependent manners.

The present study demonstrated that γδ T cells could be reproducibly proliferated from peripheral blood lymphocytes

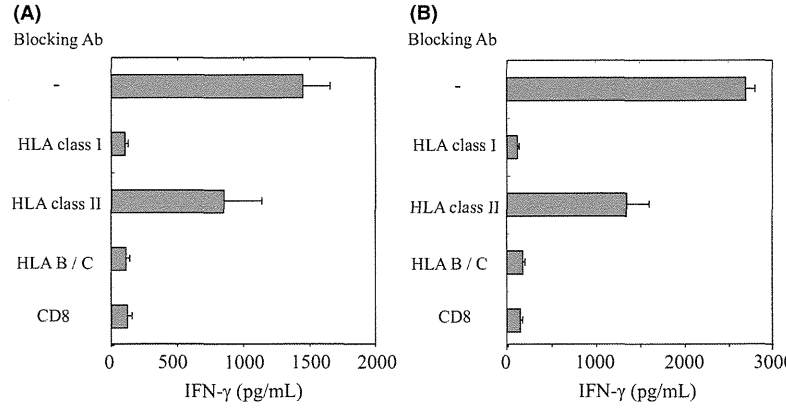

Fig. 5. Interferon-γ (IFN-γ) production of T-cell receptors (TCR) αβ-CD8 γδ T cells in response to the F1121L adenocarcinoma cell line and Epstein-Barr virus-B (EBV-B) cells pulsed with the KK-LC-1 peptide. The TCR αβ-CD8 γδT showed IFN-γ production in response to KK-LC-1-positive tumor cells as well as F1121EBV-B pulsed with KK-LC-$1_{76\text{-}84}$. The IFN-γ production was inhibited by the addition of an anti-HLA class I antibody, anti-HLA B/C antibody and anti-CD8 antibody. The stimulator was F1121L in (A) and F1121EBV-B pulsed with KK-LC-$1_{76\text{-}84}$ in (B). Results are expressed as mean ± SD.

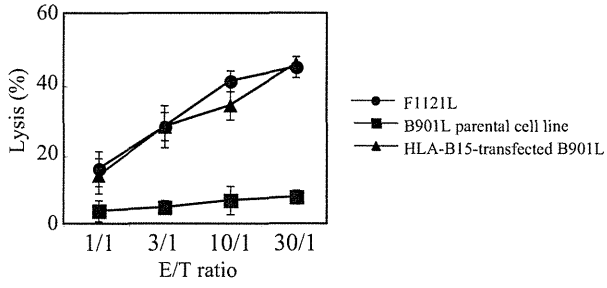

Fig. 6. Recognition of KK-LC-1-specific T-cell receptors (TCR) αβ-CD8-γδ T cells against HLA-B15-transfected B901L. A HLA-B15-positive B901L (lung adenocarcinoma cell line) was established by stable transfection of the HLA-B15 gene. The B901L-HLA-B15 cell line showed a similar susceptibility to F1121L as target cells. However, the TCRαβ-CD8 γδ T cells showed no cytotoxic activity against parental B901L. E/T, effector/target.

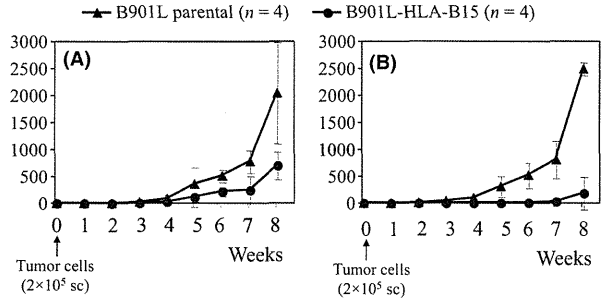

Fig. 7. Growth inhibition of B901L-HLA-B15 tumor by adoptive transfer of TCR αβ-CD8 γδ T cells. (A) Weekly intravenous injection of T-cell receptor (TCR) αβ-CD8 γδ T cells inhibited growth of the susceptible cancer cell line (B901L-HLA-B15) *in vivo*, but not for the parental cell line. (B) The twice-weekly injection of TCR αβ-CD8 γδ T cells remarkably inhibited the growth rate compared with the control cell line (parental B901L cell line). Results are expressed as mean tumor volume ± SD. sc, subcutaneous injection.

by stimulation with zoledronate. The effector cells (TCRαβ-CD8 γδ T cells) were then established from the proliferated γδ T cells by co-transduction of the TCRαβ and CD8 genes. The antigen specificity of the γδ T cells was confirmed using KK-LC-$1_{76\text{-}84}$/HLA-B15 tetramer staining. The effector cells showed tumor antigen-specific cytotoxic activity and cytokine production similar to those of the original CTL clones. However, γδ T cells transduced with TCRαβ without CD8 lost their non-specific cytotoxic activity. One of the possible causes of the decline in non-specific cytotoxic activity following the transfection of the TCRαβ genes was downregulation of the surface expression of NKG2D on the γδ T cells, because NKG2D is an important co-stimulatory molecule for γδ T cells. Intravenous injection of TCRαβ-CD8 γδ T cells inhibited growth of susceptible cancer cells (B901L-HLA-B15) *in vivo*. A histological examination revealed infiltration of TCRαβ-CD8 γδ T cells into the central part of the tumor, and the tumor subsequently became extensively necrotic. The gene transduction of TCRαβ and CD8 into γδ T cells is a promising strategy to develop a new adoptive immunotherapy against malignancies.

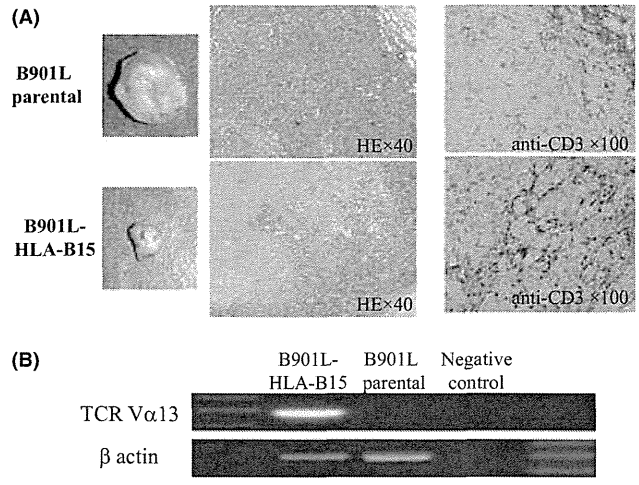

Fig. 8. Infiltration of adoptive transfer of T-cell receptor (TCR) αβ-CD8 γδT cells into the tumor. (A) Immunohistochemical staining with anti-human CD3 antibody. A large amount of CD3-positive human lymphocytes infiltrated into the B901L-HLA-B15 tumor. (B) Detection of TCR-Vα13 of TCRαβ-CD8-γδ T cells in the tumor using RT-PCR.

Cancer/testis antigens are particularly attractive targets for immunotherapy, because of their unique expression profiles that have restricted expression in testis and placental trophoblasts and male germ-line cells, which do not express HLA class I molecules and therefore cannot present the antigens to T lymphocytes.[29] Cancer/testis antigens are activated in a number of tumors of various histological types. KK-LC-1 is a cancer/testis antigen recognized by CTL. The expression rate of KK-LC-1 in patients with NSCLC is 32.6%, and the expression of KK-LC-1 is higher (32.1%) in patients with adenocarcinoma compared with other CT antigens (MAGE-A3, MAGE-A4 and NY-ESO-1).[30] KK-LC-1 might be a hopeful target for patients with adenocarcinoma, because in Japan the recent incidence of adenocarcinoma is twice that of squamous cell carcinoma.[31]

The reproducible effects of transduction of the TCRαβ gene by retroviral vector was confirmed using KK-LC-$1_{76\text{-}84}$/HLA-B15 tetramer staining. The co-transduction of TCRαβ and CD8 into these γδ T cells showed the same antigen-specific activity as an original CTL *in vitro* and *in vivo*. The gene transduction of TCRαβ and CD8 into γδ T cells is a promising strategy for developing a new adoptive immunotherapy against malignancies.

Acknowledgments

This study was supported in part by a UOEH Research Grant for the Promotion of Occupational Health and a Grant-in-Aid for scientific research from the Ministry of Education, Culture, Sports, Science and Technology, Japan. We are grateful to Professor Kosei Yasumoto for critical advice and helpful suggestions. We also thank Yukiko Koyanagi, Misako Fukumoto and Yukari Furutani for their expert technical help.

Disclosure Statement

The authors have no conflict of interest.

doi: 10.1111/j.1349-7006.2012.02337.x

References

1 Jemal A, Siegel R, Xu J, Ward E. Cancer statistics, 2010. *CA Cancer J Clin* 2010; **60**: 277–300.
2 Sangha R, Butts C. L-BLP25: a peptide vaccine strategy in non small cell lung cancer. *Clin Cancer Res* 2007; **13**: S4652–4.
3 Kimura H, Iizasa T, Ishikawa A *et al.* Prospective phase II study of post-surgical adjuvant chemo-immunotherapy using autologous dendritic cells and activated killer cells from tissue culture of tumor-draining lymph nodes in primary lung cancer patients. *Anticancer Res* 2008; **28**: 1229–38.
4 Mellstedt H, Vansteenkiste J, Thatcher N. Vaccines for the treatment of non-small cell lung cancer: investigational approaches and clinical experience. *Lung Cancer* 2011; **73**: 11–7.
5 Dudley ME, Wunderlich JR, Yang JC *et al.* Adoptive cell transfer therapy following non-myeloablative but lymphodepleting chemotherapy for the treatment of patients with refractory metastatic melanoma. *J Clin Oncol* 2005; **23**: 2346–57.
6 Schaft N, Willemsen RA, de Vries J *et al.* Peptide fine specificity of anti-glycoprotein 100 CTL is preserved following transfer of engineered TCR alpha beta genes into primary human T lymphocytes. *J Immunol* 2003; **170**: 2186–94.
7 Bonneville M, O'Brien RL, Born WK. Gammadelta T cell effector functions: a blend of innate programming and acquired plasticity. *Nat Rev Immunol* 2010; **10**: 467–78.
8 Kondo M, Izumi T, Fujieda N *et al.* Expansion of human peripheral blood γδ T cells using zoledronate. *J Vis Exp* 2011; **pii**: 3182.
9 Fukuyama T, Hanagiri T, Takenoyama M *et al.* Identification of a new cancer/germline gene, KK-LC-1, encoding an antigen recognized by autologous CTL induced on human lung adenocarcinoma. *Cancer Res* 2006; **66**: 4922–8.
10 Sugaya M, Takenoyama M, Osaki T *et al.* Establishment of 15 cancer cell lines from patients with lung cancer and the potential tools for immunotherapy. *Chest* 2002; **122**: 282–8.
11 Szymczak AL, Workman CJ, Wang Y *et al.* Correction of multi-gene deficiency *in vivo* using a single 'self-cleaving' 2A peptide-based retroviral vector. *Nat Biotechnol* 2004; **22**: 589–94.
12 Kitamura T, Koshino Y, Shibata F *et al.* Retrovirus-mediated gene transfer and expression cloning: powerful tools in functional genomics. *Exp Hematol* 2003; **11**: 1007–14.
13 Sugaya M, Takenoyama M, Shigematsu Y *et al.* Identification of HLA-A24 restricted shared antigen recognized by autologous cytotoxic T lymphocytes from a patient with large cell carcinoma of the lung. *Int J Cancer* 2007; **120**: 1055–62.
14 Rosenberg SA, Yang JC, Restifo NP. Cancer immunotherapy: moving beyond current vaccines. *Nat Med* 2004; **10**: 909–15.
15 Wright SE, Rewers-Felkins KA, Quinlin IS *et al.* Number of treatment cycles influences development of cytotoxic T cells in metastatic breast cancer patients – a phase I/II study. *Immunol Invest* 2010; **39**: 570–86.
16 Melief CJ, Toes RE, Medema JP, van der Burg SH, Ossendorp F, Offringa R. Strategies for immunotherapy of cancer. *Adv Immunol* 2000; **75**: 235–82.
17 Morgan RA, Dudley ME, Yu YY *et al.* High efficiency TCR gene transfer into primary human lymphocytes affords avid recognition of melanoma tumor antigen glycoprotein 100 and does not alter the recognition of autologous melanoma antigens. *J Immunol* 2003; **171**: 3287–95.
18 Hiasa A, Hirayama M, Nishikawa H *et al.* Long-term phenotypic, functional and genetic stability of cancer-specific T-cell receptor (TCR) alphabeta genes transduced to CD8 + T cells. *Gene Ther* 2008; **15**: 695–9.
19 Hughes MS, Yu YY, Dudley ME *et al.* Transfer of a TCR gene derived from a patient with a marked antitumor response conveys highly active T-cell effector functions. *Hum Gene Ther* 2005; **16**: 457–72.
20 Thomas S, Hart DP, Xue SA, Cesco-Gaspere M, Stauss HJ. T-cell receptor gene therapy for cancer: the progress to date and future objectives. *Expert Opin Biol Ther* 2007; **7**: 1207–18.
21 Cohen CJ, Li YF, El-Gamil M, Robbins PF, Rosenberg SA, Morgan RA. Enhanced antitumor activity of T cells engineered to express T-cell receptors with a second disulfide bond. *Cancer Res* 2007; **67**: 3898–903.
22 Okamoto S, Mineno J, Ikeda H *et al.* Improved expression and reactivity of transduced tumor-specific TCRs in human lymphocytes by specific silencing of endogenous TCR. *Cancer Res* 2009; **69**: 9003–11.
23 Jitsukawa S, Faure F, Lipinski M, Triebel F, Hercend T. A novel subset of human lymphocytes with a T cell receptor-gamma complex. *J Exp Med* 1987; **166**: 1192–7.
24 Yoshida Y, Nakajima J, Wada H, Kakimi K. γδ T-cell immunotherapy for lung cancer. *Surg Today* 2011; **41**: 606–11.
25 Todaro M, D'Asaro M, Caccamo N *et al.* Efficient killing of human colon cancer stem cells by gammadelta T lymphocytes. *J Immunol* 2009; **182**: 7287–96.
26 Kato Y, Tanaka Y, Tanaka H, Yamashita S, Minato N. Requirement of species-specific interactions for the activation of human γδ T cells by pamidronate. *J Immunol* 2003; **170**: 3608–13.
27 Kunzmann V, Bauer E, Feurle J, Weissinger F, Tony HP, Wilhelm M. Stimulation of γδ T cells by aminobisphosphonates and induction of antiplasma cell activity in multiple myeloma. *Blood* 2000; **96**: 384–92.
28 Hiasa A, Nishikawa H, Hirayama M *et al.* Rapid alphabeta TCR-mediated responses in gammadelta T cells transduced with cancer-specific TCR genes. *Gene Ther* 2009; **16**: 620–8.
29 Jungbluth AA, Busam KJ, Kolb D *et al.* Expression of MAGE-antigens in normal tissues and cancer. *Int J Cancer* 2000; **85**: 460–5.
30 Shigematsu Y, Hanagiri T, Shiota H *et al.* Clinical significance of cancer/testis antigens expression in patients with non-small cell lung cancer. *Lung Cancer* 2010; **68**: 105–10.
31 Asamura H, Goya T, Koshiishi Y *et al.* A Japanese Lung Cancer Registry study: prognosis of 13,010 resected lung cancers. *J Thorac Oncol* 2008; **3**: 46–52.

Ann Thorac Cardiovasc Surg Advance Published Date: August 20, 2012

doi: 10.5761/atcs.oa.11.01867

Original Article

Effective Utilization of Chest X-ray for Follow-up of Metastatic Lung Tumor due to Soft Tissue Sarcoma

Yasunori Shikada, MD, PhD, Tokujiro Yano, MD, PhD, Riichiro Maruyama, MD, PhD, Mitsuhiro Takenoyama, MD, PhD, and Yoshihiko Maehara, MD, PhD

Computed tomography (CT) is widely used for follow-up of lung metastasis in patients due to soft tissue sarcoma (STS), the frequency of chest X-ray (CXR) is obviously reduced. This study verified the current status of diagnostic measures and the efficacy of CXR.

A retrospective analysis of 18 patients that underwent surgery for lung metastasis due to STS was performed. The investigation compared the follow-up interval using CT after STS surgery, time from STS surgery to lung metastasis, tumor size of lung metastasis, detection rate with CXR, time from detection to surgery for lung metastasis, number of CT scans and follow-up interval using CT after detection of lung metastasis.

The follow-up interval when using CT after STS surgery was 3.5 months (m). Time from STS surgery to lung metastasis was 34.3m. Tumor size of lung metastasis was 15 mm, and the detection rate by CXR was 66.7%. The time from detection to surgery for lung metastasis was 4.8m, the number of CT scans was 3.1, and the interval was markedly shortened to 1.6m.

Follow-up should be performed by CXR if the tumor is detected by CXR. CT evaluation is required when the tumor size has increased, and prior to surgery for lung metastasis.

Keywords: soft tissue sarcoma, lung metastasis, follow-up

Introduction

Soft tissue sarcomas (STS) are rare tumors in adulthood, and STSs are a heterogenous group of malignant tumors with more than 50 histological subtypes.[1] The pattern of spread to the lungs is commonly haematogeneous.[2] In metastatic STS, the lung is the most frequent organ affected and is seen 20% of patients, which is less than that in osteosarcoma.[3] Prognostic indicators for recurrence include age at diagnosis, tumor depth, tumor size, histological type and grade, and positive surgical margins.[4–8] Imaging of the chest by computed tomography (CT) and chest X-ray (CXR) is recommended regularly for detecting the presence of pulmonary metastasis after curative resection for STS.

Computed tomography is widely used for follow-up of lung metastasis in patients with STS. On the other hand, the frequency of CXR is obviously reduced. The effective radiation dose from CXR is estimated to be between 0.02 mSv and 0.1 mSv, which is equivalent to between 2.4 days and 10 days of background radiation. Obviously, the overall radiation dose of CXR is smaller than that of CT. Furthermore, CT may give false positive results in the presence of small lung nodules (<5 mm).[9]

Although CXR is a valid and feasible way, CT is performed without CXR.

The aim of this study is to elucidate the current status of diagnostic measures for the follow-up of lung metastasis due to STS and the efficacy of CXR.

Department of Surgery and Science, Graduate School of Medical Sciences, Kyushu University, Fukuoka, Japan

Received: December 12, 2011; Accepted: February 28, 2012
Corresponding author: Yasunori Shikada, MD, PhD. Department of Surgery and Science, Graduate School of Medical Sciences, Kyushu University, Maidashi 3-1-1, Higashi-ku, Fukuoka, Fukuoka 812-8582, Japan
Email: shikada0416@yahoo.co.jp

Table 1 Analysis results of all patients

Follow-up interval using CT after STS surgery	3.5m (1–24)
Time from STS surgery to lung metastasis	34.3m (1–132)
Tumor size of lung metastasis at surgery	15 mm (6–41)
Detection rate of CXR	66.7% (12/18)
Time from detection to surgery for lung metastasis	4.8m (1–23)
Number CT scans after detection	3.1 (1–15)
Follow-up interval using CT after detection	1.6m (1–4.0)

STS: soft tissue sarcoma; CXR: chest X-ray

Table 2 Results based on CXR availability

Factor	Detectable by CXR (n = 12)	Undetectable by CXR (n = 6)	p-value
Follow-up interval	3.7m (1–24)	3.1m (2–6)	N.S.
Time from STS to lung meta	30.8m (1–108)	39.8m (2–132)	N.S.
Tumor size at surgery	15 mm (6–41)	8 mm (6–10)	$p < 0.05$
Time from detection to surgery	5.0m (1–23)	4.1m (1–18)	N.S.
Number CT scans	3.5 (1–15)	2.0 (1–5)	N.S.
Follow-up interval using CT	1.4m (1–2.2)	2.1m (1–4.0)	N.S.

STS: soft tissue sarcoma; CXR: chest X-ray

Patients and methods

A retrospective analysis of consecutive 18 patients (synovial sarcoma, 6; liposarcoma, 3; malignant peripheral nerve sheath tumor, 2; leiomyosarcoma, 2; malignant fibrous histiocytoma, 2; alveolar rhabdomyosarcoma, 2; ewing sarcoma,[1]) that underwent surgery for lung metastasis due to STS during a 4-year period was performed between August 2006 and October 2010. The subjects included 9 males and 9 females with a mean age of 42.6 ± 8.6 (12 to 67) years. The study compared the follow-up interval when using CT after STS surgery, time from STS surgery to lung metastasis, tumor size of lung metastasis during surgery, detection rate with CXR, time from detection to surgery for lung metastasis, number of CT scans after detection of lung metastasis, and follow-up interval using CT after detection of lung metastasis. Informed consent was received from each patient in this study. Statistical analysis was examined using Mann-Whitney U tests.

Results

The results of the analysis of all patients are shown in **Table 1**. The follow-up interval using CT after STS surgery was 3.5 months (m; 1–24m). The time from STS surgery to lung metastasis was 34.3 m (1–132m). The median tumor size of the maximal lung metastasis was 15 mm (6–41 mm), and the detection rate by CXR was 66.7% (12/18). The time from detection to surgery for lung metastasis was 4.8 m (1–23), number of CT scans after detection of lung metastasis to surgery was 3.1 (1–15), and the interval was markedly shortened to 1.6m (1–4.0m).

Results of the analysis based on CXR availability is shown in **Table 2**. There was no statistical difference of background disease between the two groups (detectable in CXR group: synovial sarcoma, 4; liposarcoma, 2; malignant peripheral nerve sheath tumor, 1; leiomyosarcoma, 1; malignant fibrous histiocytoma, 2; alveolar rhabdomyosarcoma, 1; ewing sarcoma, 1; undetectable in CXR group: synovial sarcoma, 2; liposarcoma, 1; malignant peripheral nerve sheath tumor, 1; leiomyosarcoma, 1; alveolar rhabdomyosarcoma.[1]) The follow-up interval when using CT after STS surgery of cases detectable by CXR was 3.7 m (1–24 m), and that in cases undetectable by CXR cases was 3.1m (2–6 m). The time from STS surgery to lung metastasis of cases detectable by CXR was 30.8m (1–108 m), and time in cases undetectable by CXR was 39.8m (2–132m). Median tumor size of the maximal lung metastasis of cases detectable by CXR was 15 mm (6–41 mm), and tumor size in cases undetectable by CXR was 8 mm (6–10mm; $p < 0.05$). The time from detection to surgery of lung metastasis in cases detectable by CXR was 5.0m (1–23m), and time in cases undetectable by CXR was 4.1m (1–18m), respectively. The number of CT scans from detection of lung metastasis to surgery cases,

detectable by CXR was 3.5 (1–15m), and the number in cases undetectable by CXR was 2.0m (1–5m), respectively. Those intervals were markedly shortened to 1.4m (1–4.0m), 2.1 m (1–4.0), respectively. Although these results were based on a retrospective analysis, lung nodules that were detectable by CXR were observed by follow-up with CT within a short period of time prior to surgery to lung metastasis.

Because this study had a a small sample size and was performed during a recent 5 year period, the survival rate could not be accurately analyzed. The median survival time detectable in the CXR group was 18 months, and undetectable in the CXR group, was 16 months.

Discussion

Soft tissue sarcoma is a rare disease, a heterogeneous group of solid tumors, and arises primarily from embryonic mesoderm. Soft tissue sarcoma occurs in about 2 patients per million, in Japan. The 5-year survival for STS of all stages is between 50% and 60%.[10] Several studies on pulmonary metastectomy for STS have been published, and the 5-year survival ranges from 25% to 57%.[11–14] All these studies have shown that complete surgical resection of pulmonary metastasis is a significant prognostic factor of STS. Surgical treatment of metastatic pulmonary STS is the best procedure for cure.

Currently the most common measure for screening lung metastasis is CT. However, although CT is more accurate, the difference in accuracy is not great. The accuracy of CXR is 96.9%, in comparison to 99.6% with CT. Furthermore, CT will detect indeterminate nodules. Chalmers reported that pulmonary nodules that were not seen on a CXR detected on CT in 13% of 146 patients with extra thoracic malignancy, but 80% of these nodules were benign.[15] Computed tomography is by no means infallible, and it could be argued that the detection of indeterminate nodules may lead to unnecessary investigation. The usefulness of a routine CXR to diagnose lung metastasis in STS has been less well documented. Kane summarized that CT is associated with a lack of cost effectiveness, increased regular clinic visits and clinical examinations.[16] Change AE et al. suggested that the low cumulative dose of radiation received from 6 monthly CXRs makes this a safe, simple, and appropriate first tool.[17] Chest X-radiography will pick up these large lung lesions, and CT of the chest is not always needed. Lung lesions below 5 mm in diameter will be missed on CXR and will only be identified on CT. The vast majority of these patients is completely asymptomatic and will be offered radical surgery.

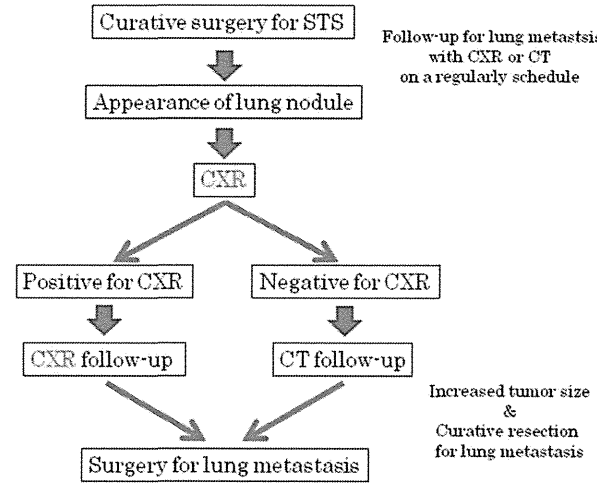

Fig. 1 Flow diagram of follow-up for lung metastasis.
Follow-up for lung metastasis with CXR or CT was performed as ever. CXR is examined if lung metastasis is detected on CT. When the tumor is detected by CXR, a follow-up is performed by CXR. When the tumor has obviously grown, it is evaluated by CT prior to surgery for lung metastasis.
CXR: chest X-ray

A recent study proposed that all patients with STS have a CXR, and only those patients with an abnormality on CXR or with a high/intermediate grade, such as deep tumors greater than 5 cm (stage 2b/3) in size, specific histological subtypes of STS, where the incidence of lung metastases at diagnosis is known to be high, for example, extra skeletal ewing sarcoma and malignant peripheral nerve sheath tumor, should undergo a CT routinely.[18]

The goal of this study was to evaluate the current status of diagnostic measures to follow-up of lung metastasis due to STS and the efficacy of CXR. Most patients in this study were followed by routine CT only, but not by CXR. The results revealed that metastatic pulmonary nodules were detectable by CXR (66.7%), nodules undetectable by CXR were smaller than 10 mm. The time from detection to surgery was 4.8 m. The mean number of follow-up CT scans during this period was 3.1, and this interval was markedly short (1.6m).

This study confirmed that CT has been extensively used in the follow-up examination of lung metastasis due to STS. Orthopedists employ follow-up using CT regularly, since they feel insecure in follow-up only by CXR. We suggest the method of follow-up examination in **Fig. 1**.

A pulmonary nodule that cannot be detected by CXR requires the use of CT scans during the follow-up examination. However, pulmonary nodules that can be detected by CXR should be followed with the combined use of CXR and CT until the resection.

This study is a limited, small number study, but STS is a heterogenous malignant subtype group. Furthermore, we will validate the effectiveness of CXR for follow-up of various metastatic lung tumors. In the present study, we showed that CXR provided much information for follow-up of metastatic lung tumor due to soft tissue sarcoma. In conclusion, it is important for clinicians to utilize CXR effectively while understanding the limit and characteristic of the modality, enough.

Disclosure Statement

No author has any conflict of interest

References

1) van Vliet M, Kliffen M, Krestin GP, et al. Soft tissue sarcomas at a glance: clinical, histological, and MR imaging features of malignant extremity soft tissue tumors. Eur Radiol 2009; **19**: 1499-511.
2) Billingsley KG, Lewis JJ, Leung DH, et al. Multifactorial analysis of the survival of patients with distant metastasis arising from primary extremity sarcoma. Cancer 1999; **85**: 389-95.
3) van Geel AN, Pastorino U, Jauch KW, et al. Surgical treatment of lung metastases: The European Organization for Research and Treatment of Cancer-Soft Tissue and Bone Sarcoma Group study of 255 patients. Cancer 1996; **77**: 675-82.
4) Le Doussal V, Coindre JM, Leroux A, et al. Prognostic factors for patients with localized primary malignant fibrous histiocytoma: a multicenter study of 216 patients with multivariate analysis. Cancer 1996; **77**: 1823-30.
5) Le QT, Fu KK, Kroll S, et al. Prognostic factors in adult soft-tissue sarcomas of the head and neck. Int J Radiat Oncol Biol Phys 1997; **37**: 975-84.
6) Coindre JM, Terrier P, Guillou L, et al. Predictive value of grade for metastases development in the main histologic types of adult soft tissue sarcomas: a study of 1240 patients from the French Federation of Cancer Centers Sarcoma Group. Cancer 2001; **91**: 1914-26.
7) Vraa S, Keller J, Nielsen OS, et al. Prognostic factors in soft tissue sarcomas: the Aarhus experience. Eur J Cancer 1998; **34**: 1876-82.
8) Collin CF, Friedrich C, Godbold J, et al. Prognostic factors for local recurrence and survival in patients with localized extremity soft-tissue sarcoma. Semin Surg Oncol 1988; **4**: 30-7.
9) Davis SD. CT evaluation for pulmonary metastases in patients with extrathoracic malignancy. Radiology 1991; **180**: 1-12.
10) Pisters P. Staging and prognosis. In: Pollock RE, editor. American Cancer Society atlas of clinical oncology: soft tissue sarcoma. Hamilton, Ontario: BC Decker Inc., 2002; pp80-8.
11) van Geel AN, van Coevorden F, Blankensteijn JD, et al. Surgical treatment of pulmonary metastases from soft tissue sarcomas: a retrospective study in The Netherlands. J Surg Oncol 1994; **56**: 172-7.
12) Billingsley KG, Burt ME, Jara E, et al. Pulmonary metastases from soft tissue sarcoma: analysis of patterns of diseases and postmetastasis survival. Ann Surg 1999; **229**: 602-10; discussion 610-2.
13) Chen F, Fujinaga T, Sato K, et al. Significance of tumor recurrence before pulmonary metastasis in pulmonary metastasectomy for soft tissue sarcoma. Eur J Surg Oncol 2009; **35**: 660-5.
14) Pfannschmidt J, Klode J, Muley T, et al. Pulmonary metastasectomy in patients with soft tissue sarcomas: experiences in 50 patients. Thorac Cardiovasc Surg 2006; **54**: 489-92.
15) Chalmers N, Best JJ. The significance of pulmonary nodules detected by CT but not by chest radiography in tumour staging. Clin Radiol 1991; **44**: 410-2.
16) Kane JM 3rd. Surveillance strategies for patients following surgical resection of soft tissue sarcomas. Curr Opin Oncol 2004; **16**: 328-32.
17) Chang AE, Schaner EG, Conkle DM, et al. Evaluation of computed tomography in the detection of pulmonary metastases: a prospective study. Cancer 1979; **43**: 913-6.
18) Lord HK, Salter DM, MacDougall RH, et al. Is routine chest radiography a useful test in the follow up of all adult patients with soft tissue sarcoma? Br J Radiol 2006; **79**: 799-800.

First Case of Combined Small-Cell Lung Cancer with Adenocarcinoma Harboring *EML4-ALK* Fusion and an Exon 19 *EGFR* Mutation in Each Histological Component

Gouji Toyokawa, MD, PhD, Kenichi Taguchi, MD, PhD,† Taro Ohba, MD, PhD,* Yosuke Morodomi, MD, PhD,* Tomoyoshi Takenaka, MD, PhD,* Fumihiko Hirai, MD, PhD,* Masafumi Yamaguchi, MD, PhD,* Takashi Seto, MD, PhD,* Mitsuhiro Takenoyama, MD, PhD,* Kenji Sugio, MD, PhD, FACS,* and Yukito Ichinose, MD, PhD**

A 72-year-old male exsmoker of 60-pack-years had undergone a high anterior resection, followed by chemotherapy (Leucovorin+5-Fluorouracil, S-1, FOLFOX-4+Bevacizumab, FOLFIRI+Bevacizumab) for rectal cancer with liver and sacral bone metastases 6 years ago. Because a nodal shadow had appeared in the right lower lobe of the lung, despite the disappearance of the liver and sacral metastases, he was referred to our department for a treatment of the pulmonary nodule.

Computed tomography showed an irregular nodule in the right lower lobe, which was confirmed as active by positron emission tomography, although there were no active lesions on the liver or sacral bone (Fig. 1*A*). The pulmonary lesion was assumed to be primary lung cancer, and right lower lobectomy with lymphadenectomy was performed. The cut sections revealed a whitish solid nodule encircled by a gray-whitish component with a maximum diameter of 4.5 cm (Fig. 1*B*). The central component was pathologically diagnosed as small-cell lung cancer (SCLC), which was 30% of the entire tumor, and the surrounding area was adenocarcinoma (70%) with papillary, acinar and lepidic components (formerly nonmucinous bronchioloalveolar carcinoma, 10%; Fig. 2 *A– C*). Both the components showed immunoreactivity to thyroid transcriptional factor 1, whereas synaptophysin and CD56 were detected only in the SCLC component. The pathological stage was finally determined to be IB. Each of the components was separately examined for mutations of epidermal growth factor receptor (*EGFR*) and anaplastic lymphoma kinase (*ALK*) by the direct sequencing method. A deletion in exon 19 of *EGFR* was detected only in the lepidic component, whereas only the SCLC component harbored variant 1 of echinoderm microtubule-associated protein-like 4 (*EML4*)-*ALK* fusion (Fig. 3*A*, *B*) and those were confirmed by immunohistochemistry (Fig. 3*C*, *D*). Figure. 3*E* shows gene mapping of the mutations in each component.

DISCUSSION

Gene mutations in tyrosine kinases play crucial roles in the pathogenesis of adenocarcinoma. Tumors with the *EGFR* gene, the most well-known tyrosine kinase which

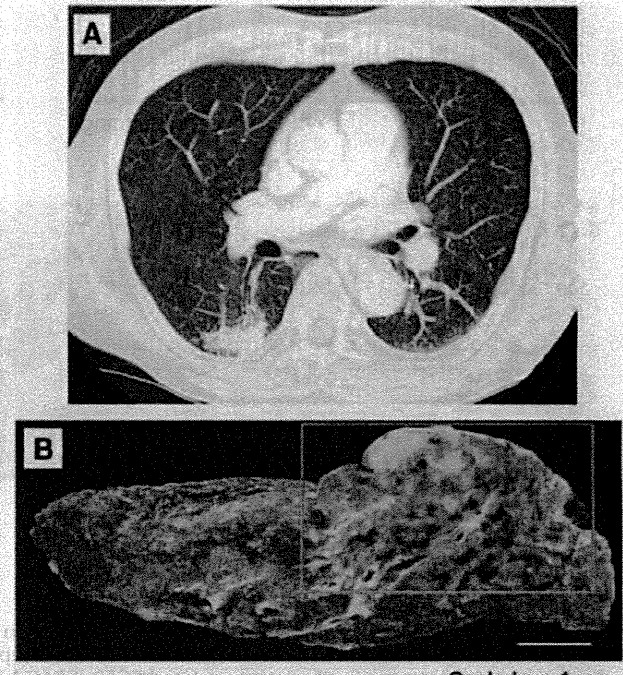

FIGURE 1. *A*, Computed tomography showing an irregular nodule in the right lower lobe of lung. *B*, Cut sections of the tumor are seen by the encircled part.

*Department of Thoracic Oncology, National Kyushu Cancer Center, Fukuoka, Japan; and †Cancer Pathology Laboratory, Clinical Research Institute, National Kyushu Cancer Center, Fukuoka, Japan.

Disclosure: The authors declare no conflict of interest.

Address for correspondence: Kenji Sugio, Department of Thoracic Oncology, National Kyushu Cancer Center, 3-1-1 Notame, Minami-ku, Fukuoka 811–1395, Japan. E-mail: sugio.k@nk-cc.go.jp

ISSN: 1556-0864/12/0712-e39

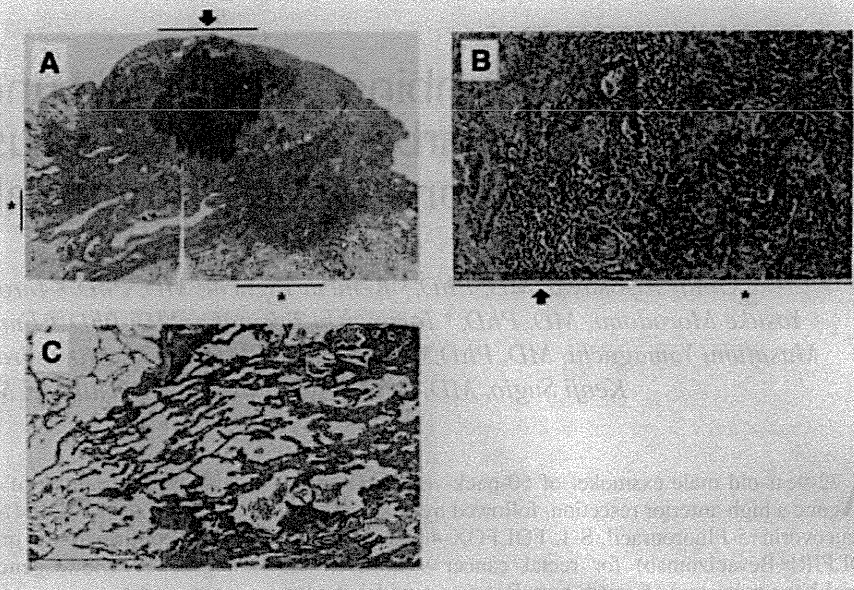

FIGURE 2. Microscopic findings. *A*, Microscopic findings of the tumor consisting of SCLC (arrow) surrounded by adenocarcinoma with papillary, acinar and lepidic components (asterisk). Highly magnified images of (*B*) the SCLC (asterisk), the adenocarcinoma (arrow), and (*C*) the lepidic components. SCLC, small-cell lung cancer.

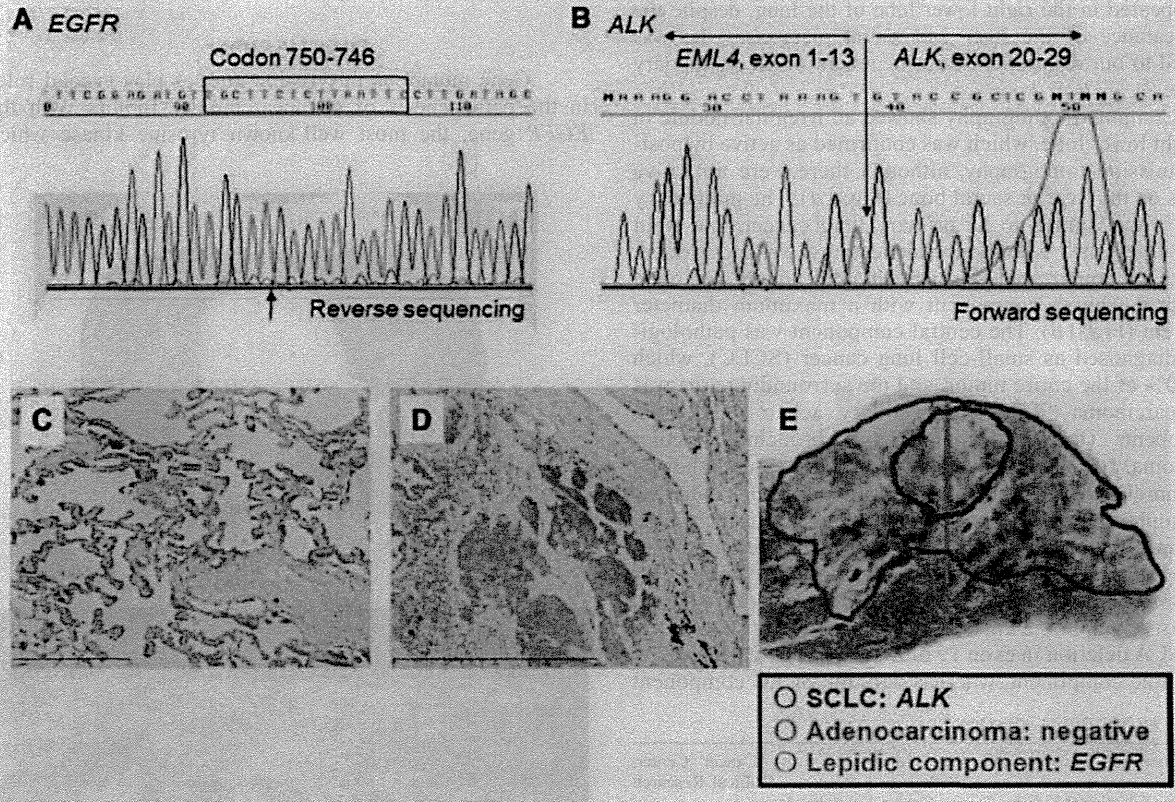

FIGURE 3. A direct sequence analysis revealing (*A*) a deletion in exon 19 of *EGFR* in the adenocarcinoma and (*B*) a variant 1 mutation of *EML4-ALK* in the SCLC. Immunoreactivity of the lepidic component to the deletion in exon 19 of EGFR using an antibody that specifically detects deleted EGFR (E746-A750del) (6B6, Cell Signaling, Danvers, MA) (*C*) and of the SCLC to ALK using primary antibody against ALK (5A4, Nichirei, Tokyo, Japan) (*D*). A polymer method was used for the immunohistochemical analysis, specifically, an intercalating antibody-enhanced polymer method was used for the detection of ALK. *E*, Gene mapping of the driver mutations in each component. EGFR, epidermal growth factor receptor; EML4-ALK, echinoderm microtubule-associated protein-like 4; SCLC, small-cell lung cancer; ALK, anaplastic lymphoma kinase.

harbors activating mutations in exon 19 and 21, can be successfully treated by EGFR-tyrosine kinase inhibitors (TKIs) in comparison to cytotoxic reagents.[1] The *EML4-ALK* fusion gene also possesses a transforming activity[2] and has attracted much attention because it might be a potential therapeutic target of ALK inhibitors in the treatment of adenocarcinoma.[3] Although *EGFR* mutations have already been identified in SCLCs (4%),[4] there are no reports on the *EML4-ALK* translocation in SCLCs. Intriguingly, *ALK* translocation was detected in the SCLC component in the present case, whereas the exon 19 *EGFR* mutation was shown only in the lepidic component.

Adenocarcinoma with sensitive *EGFR* mutations can transform into SCLC in the process of acquiring resistance to EGFR-TKIs.[5] This mechanism does not apply to the current case, because the patient had not received EGFR-TKIs. Although the complexity of the combined histology and driver mutations in the present case has not been elucidated, this phenomenon suggests that *ALK* rearrangements could be involved in the pathogenesis of SCLC, which could be successfully treated with ALK inhibitors.

REFERENCES

1. Mitsudomi T, Morita S, Yatabe Y, et al.; West Japan Oncology Group. Gefitinib versus cisplatin plus docetaxel in patients with non-small-cell lung cancer harbouring mutations of the epidermal growth factor receptor (WJTOG3405): an open label, randomised phase 3 trial. *Lancet Oncol* 2010;11:121–128.
2. Soda M, Choi YL, Enomoto M, et al. Identification of the transforming EML4-ALK fusion gene in non-small-cell lung cancer. *Nature* 2007;448:561–566.
3. Scagliotti G, Stahel RA, Rosell R, Thatcher N, Soria JC. ALK translocation and crizotinib in non-small cell lung cancer: an evolving paradigm in oncology drug development. *Eur J Cancer* 2012;48:961–973.
4. Tatematsu A, Shimizu J, Murakami Y, et al. Epidermal growth factor receptor mutations in small cell lung cancer. *Clin Cancer Res* 2008;14:6092–6096.
5. Sequist LV, Waltman BA, Dias-Santagata D, et al. Genotypic and histological evolution of lung cancers acquiring resistance to EGFR inhibitors. *Sci Transl Med* 2011;3:75ra26.

Int Canc Conf J
DOI 10.1007/s13691-012-0068-4

CASE REPORT

Cystic brain metastasis of non-small-cell lung cancer successfully controlled with Ommaya reservoir placement

Gouji Toyokawa · Ryo Toyozawa · Eiko Inamasu · Miyako Kojo · Yosuke Morodomi · Yoshimasa Shiraishi · Tomoyoshi Takenaka · Fumihiko Hirai · Masafumi Yamaguchi · Takashi Seto · Mitsuhiro Takenoyama · Yukito Ichinose

Received: 7 August 2012 / Accepted: 23 October 2012

Abstract A 68-year-old male presented with hoarseness and anarthria. Computed tomography showed an irregular nodular shadow in the upper lobe of the left lung with swollen multiple lymph nodes. Magnetic resonance imaging revealed a large cystic mass in the left hemisphere of the brain and multiple brain metastases in the bilateral hemispheres. A direct biopsy with bronchoscopy of the pulmonary nodule revealed the tumor to be an adenocarcinoma clinically diagnosed as stage IV. Since the largest brain metastasis continued to grow despite the administration of whole brain irradiation, insertion of an Ommaya reservoir in the cystic lesion was performed. This resulted in a reduction of the size of the brain tumor, and the patient's neurological symptoms improved. After the Ommaya reservoir was placed, stereotactic radiosurgery was performed on the largest lesion. The patient is doing well at 6 months after the Ommaya reservoir was inserted and is currently undergoing chemotherapy. In conclusion, the placement of an Ommaya reservoir may therefore be a potentially useful therapeutic procedure to improve the neurological symptoms and performance status in non-small-cell lung cancer patients with cystic brain metastasis, thereby allowing further neurosurgical therapy and chemotherapy.

Keywords Non-small-cell lung cancer · Cystic brain metastasis · Ommaya reservoir

G. Toyokawa (✉) · R. Toyozawa · E. Inamasu · M. Kojo · Y. Morodomi · Y. Shiraishi · T. Takenaka · F. Hirai · M. Yamaguchi · T. Seto · M. Takenoyama · Y. Ichinose
Department of Thoracic Oncology, National Kyushu Cancer Center, 3-1-1 Notame, Minami-ku, Fukuoka 811-1395, Japan
e-mail: gouji104kawa@gmail.com

Introduction

An Ommaya reservoir is a device placed under the skin of the head with the tip of the catheter positioned into the ventricles or within cystic lesions in the brain [1]. This device helps to drain the cerebrospinal fluid and contents of cystic lesions. Additionally, intraventricular administration of some drugs, such as amphotericin B, primethamine and methotrexate, can be conducted through this device [1, 2]. Although the usefulness of this device for treating cystic lesions in the brain has been previously reported, few reports of cystic brain metastases from lung cancer being controlled by the insertion of an Ommaya reservoir have been published in the English literature [3, 4]. In this report, we present a case of non-small-cell lung cancer (NSCLC) with a large cystic brain metastasis that was successfully controlled with the insertion of an Ommaya reservoir.

Case report

A 68-year-old male ex-smoker was referred to our hospital due to hoarseness and anarthria. Computed tomography (CT) revealed an irregular nodular shadow in the left upper lobe of the lung with enlargement of the left hilar, para-aortic and left subclavicular lymph nodes, which showed abnormal uptake of F-18 fluorodeoxyglucose on positron emission tomography/computed tomography (Fig. 1a). Magnetic resonance imaging (MRI) revealed a large mass in the left hemisphere (Fig. 1b, c) and multiple small nodules in the bilateral hemispheres (Fig. 1b, arrow). T1-weighted images showed very low signal intensity and T2-weighted images showed very high signal intensity in the largest mass consistent with the findings of a cystic lesion.

Published online: 21 November 2012

Bronchoscopy was then performed and a direct biopsy revealed the tumor to be an adenocarcinoma. Based on these findings, the clinical stage was considered to be stage IV (cT1bN3M1b).

Due to the presence of multiple brain metastases with the one larger than 3 cm, 30 Gray (Gy) of whole brain irradiation (WBI) was administered. Despite the administration of WBI, the largest cystic tumor continued to grow, and the surrounding edema expanded and the midline shifted (Fig. 1d). This resulted in worsened anarthria and the emergence of Gerstmann's syndrome. Various neurosurgical procedures were considered, and insertion of an Ommaya reservoir was chosen to minimize invasiveness. A dome-shaped plastic device was placed under the skin of the left head with a catheter positioned into the cavity of the cystic lesion without any complications (Fig. 2a). MRI and CT performed about 1 month after MRI as shown in Fig. 1c, revealed a reduction in the size of the tumor and the amount of surrounding edema (Fig. 2b, c). Crucially, the neurological symptoms improved. Since the cystic tumor was reduced from 4.7 to 2.9 cm, 20 Gy of stereotactic radiosurgery (SRS) was administered. Although the cystic tumor remained the same size after the SRS was completed, no punctures were needed to drain the fluid. The patient is doing well at 6 months after the insertion of the Ommaya reservoir and is currently undergoing chemotherapy with carboplatin and pemetrexed due to the improvement of performance status (PS) from 3 to 1.

Discussion

Ommaya reservoirs were originally developed to achieve aseptic access to ventricular cerebrospinal fluid. The device consists of an indwelling subcutaneous capsule made of silicone rubber that fits into a cranial burr-hole and is connected to a ventricular catheter. Percutaneous needle punctures can be repeatedly made through the dome of the capsule. This device is used for the administration of chemotherapy for neoplasia, cystic tumor drainage, ventricular drainage, special diagnostic studies and sampling of cerebrospinal fluid [1, 2]. In addition, diverse types of diseases, such as primary brain tumors, fungal meningitis, toxoplasmosis and head injury, can be indications for the placement of the device [1]. However, few reports of cystic brain metastasis from lung cancer being controlled with the

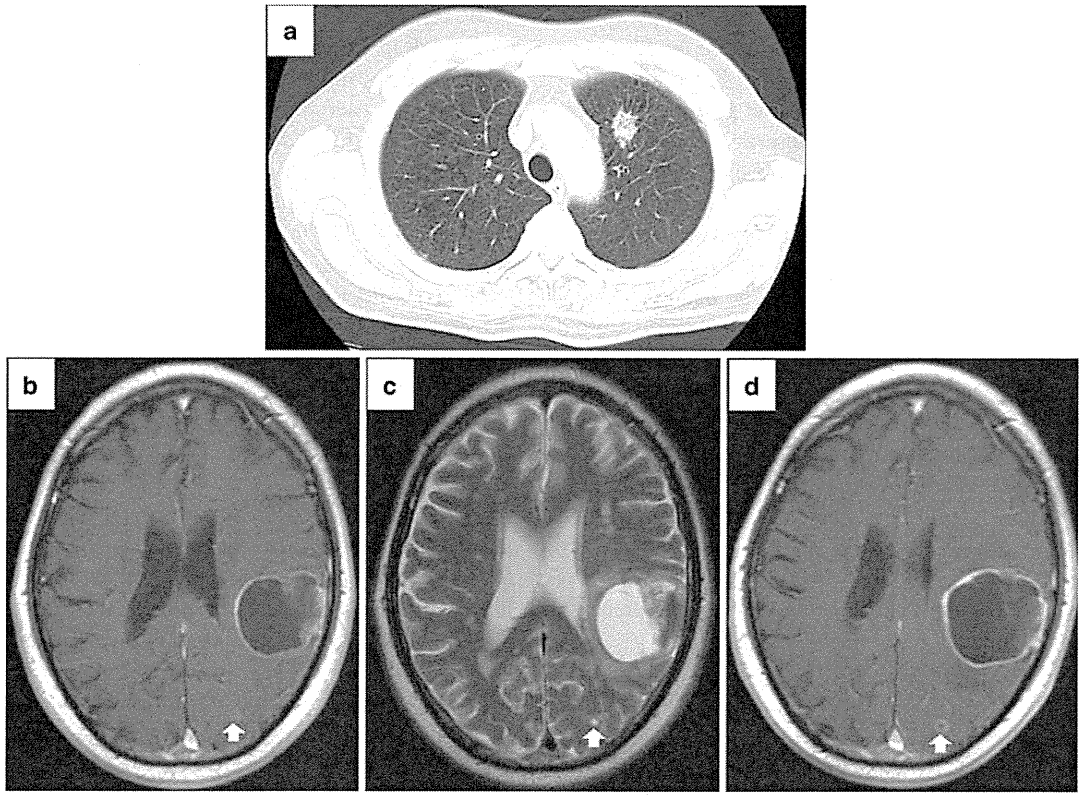

Fig. 1 CT and MRI findings. CT shows an irregular nodule in the left upper lobe of the lung (**a**). T1- and T2-weighted images indicate a large cystic brain tumor and multiple small cystic nodules (*arrow*) before the administration of WBI (**b**, **c**). T1-weighted images show the tumor after WBI (**d**)

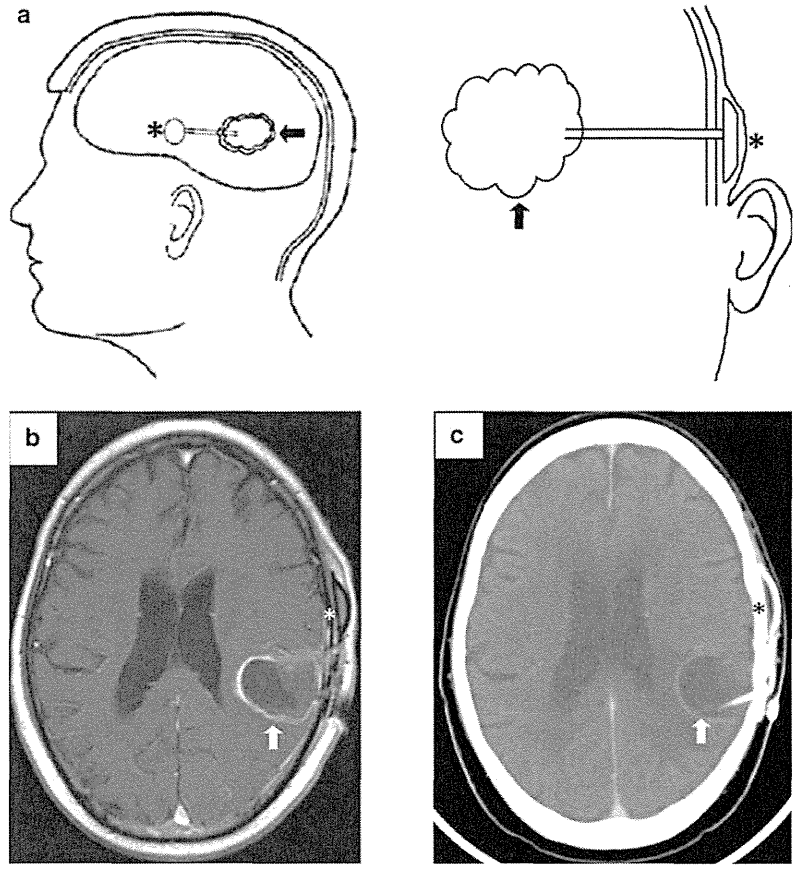

Fig. 2 Ommaya reservoir placement. Left lateral and frontal views of the head show the Ommaya reservoir (*asterisk*) placed under the skin of the left head with a catheter positioned into the cavity of the cystic lesion (*arrow*) (**a**). MRI and CT images show the inserted Ommaya reservoir (**b**, *asterisk*, **c**)

insertion of an Ommaya reservoir have been published in the English literature [3, 4]. Takeda and colleagues reported the case of a SCLC patient with solitary cystic brain metastasis who was successfully treated with a stereotactically inserted Ommaya reservoir followed by neurosurgical resection of the tumor, and the survival time of the patient after the insertion of the device was 4 months [3]. In addition, the usefulness of SRS following Ommaya reservoir placement has been reported in patients with large cystic metastatic brain tumors, including lung and breast cancer, with a median survival time of 7 months after the insertion of the device [4]. However, these papers did not mention chemotherapy after an Ommaya reservoir was placed. In the present case, a metastasized cystic lesion of the brain was controlled with the insertion of an Ommaya reservoir followed by the administration of stereotactic radiosurgery and chemotherapy, and the patient is currently doing well at 6 months, in comparison to the findings reported by others [3, 4], after the insertion of the device. Chemotherapy, as well as the insertion of the device, was also thought to have contributed the survival time of the patient, because the primary lesions and the metastasized lymph nodes were reduced after the administration of four cycles of carboplatin and pemetrexed.

Brain metastases are common in lung cancer patients, with an incidence of approximately 40 %. The majority of brain metastases of NSCLC are solid, whereas cystic brain metastases are exceedingly rare. While solid brain metastases are treated with optimal treatment modalities such as WBI, SRS or neurological surgery depending on the size and number of the metastases and the general conditions of the patient, cystic counterparts are generally resistant to radiation therapy, and neurosurgery of cystic lesions has been reported to be preferable to SRS or stereotactic aspiration when possible [5]. However, in the present case, due to the presence of multiple metastatic lesions, WBI was first chosen followed by insertion of an Ommaya reservoir for less invasiveness and to achieve ventricular drainage and drainage of the primary brain cystic tumors [1]. It is of note that no punctures were needed to drain the cystic tumors, as several punctures are generally required since the effusion typically fills the mass [3]. This may have been due to the reduction of viable cancer cells in the cystic wall by the multimodal treatments. Additionally,

although few complications are associated with the placement of the device, attention should be paid to potential adverse events caused by chemotherapy, including leucopenia, neutropenia and thrombocytopenia by chemotherapy, which can lead to critical complications such as intracranial hemorrhage or infection.

In conclusion, the insertion of an Ommaya reservoir is therefore considered to be a useful treatment modality to improve the neurological symptoms and PS in NSCLC patients with cystic brain metastasis with minimal invasiveness, thus allowing for the administration of further neurosurgical therapy and chemotherapy which are crucial for the successful treatment of advanced NSCLC.

Conflict of interest No authors have any conflict of interest to disclose.

References

1. Ratcheson RA, Ommaya AK (1968) Experience with the subcutaneous cerebrospinal-fluid reservoir. Preliminary report of 60 cases. N Engl J Med 279:1025–1031
2. Witorsch P, Williams TW Jr, Ommaya AK et al (1965) Intraventricular administration of amphotericin B. Use of subcutaneous reservoir in four patients with mycotic meningitis. JAMA 194: 699–702
3. Takeda T, Saitoh M, Takeda S (2009) Solitary cystic brain metastasis of small-cell lung carcinoma controlled by a stereotactically inserted Ommaya reservoir. Am J Med Sci 337:215–217
4. Yamanaka Y, Shuto T, Kato Y et al (2006) Ommaya reservoir placement followed by Gamma Knife surgery for large cystic metastatic brain tumors. J Neurosurg 105:79–81
5. Kim MS, Lee SI, Sim SH (1999) Brain tumors with cysts treated with Gamma Knife radiosurgery: is microsurgery indicated? Stereotact Funct Neurosurg 72:38–44

Lung Cancer 79 (2013) 118–124

Contents lists available at SciVerse ScienceDirect

Lung Cancer

journal homepage: www.elsevier.com/locate/lungcan

Distinctive histopathological features of lepidic growth predominant node-negative adenocarcinomas 3–5 cm in size

Yusuke Takahashi[a,b,c], Genichiro Ishii[b,*], Keiju Aokage[a], Tomoyuki Hishida[a], Junji Yoshida[a], Kanji Nagai[a]

[a] Division of Thoracic Oncology, National Cancer Center Hospital East, Kashiwa, Chiba, Japan
[b] Pathology Division, Research Center for Innovative Oncology, National Cancer Center Hospital East, Kashiwa, Chiba, Japan
[c] Division of General Thoracic Surgery, Tokyo Metropolitan Cancer and Infectionus Disease Center, Komagome Hospital, Bunkyo-ku, Tokyo, Japan

ARTICLE INFO

Article history:
Received 30 July 2012
Received in revised form 23 October 2012
Accepted 26 October 2012

Keywords:
Adenocarcinoma
Lepidic growth component
Vascular invasion
Pleural invasion
Prognostic indicator
Collapse area

ABSTRACT

Introduction: Adenocarcinoma of the lung is a morphologically heterogeneous group of tumors which includes a variable portion of different histologic subtype components: lepidic growth (LG), and acinar, papillary and solid subtypes. Among these, LG is a non-invasive component which is one of the major histological subtypes in small-sized adenocarcinoma (2 cm or less). However, in large adenocarcinomas (3–5 cm in size), the clinicopathological significance of LG components remains unclear.
Methods: A series of 135 lung adenocarcinomas 3–5 cm in size, without lymph node involvement, were reviewed and classified according to their percentage of LG components. We examined the correlation between the percentage of LG components and clinicopathological factors of these tumors.
Results: There were 41 (30.4%) tumors with 50% or more LG (LG-predominant group). Female gender ($p = 0.039$), smoking history of <20 pack-years ($p = 0.039$), absence of pleural invasion ($p = 0.003$), and absence of vascular invasion ($p < 0.001$) were significantly more frequently observed in the LG-predominant group. LG-predominant tumors showed a significantly higher percentage of non-cancerous cell collapse area to tumor area compared with non-LG predominant tumors ($p < 0.001$). The outcome of the LG-predominant type patients was significantly better than that of the non-LG predominant type patients in both recurrence-free survival ($p < 0.001$) and overall survival ($p < 0.001$). Multivariate analysis showed that LG-predominant tumor to be an independent favorable prognostic factor (HR = 0.285, 95% confidence interval: 0.148–0.547, $p = 0.014$).
Conclusion: Node-negative LG-predominant adenocarcinomas of 3–5 cm in size showed less invasiveness compared to non-LG predominant tumors. And LG-predominant type patients had excellent surgical outcome.

1. Introduction

Adenocarcinoma is defined as a malignant epithelial tumor with glandular differentiation or mucin production, consisting of either bronchioloalveolar, acinar, papillary, solid with mucin growth patterns, or a mixture of these patterns. Among these, adenocarcinoma of mixed subtype is the most frequent, representing approximately 80% of surgically resected lung adenocarcinomas [1].

Bronchioloalveolar carcinoma (BAC) or a lepidic growth (LG) component, which demonstrates a replacing growth pattern within the alveolar epithelium, is generally considered to be a non-invasive component. It has been reported that LG-predominant histology is a statistically significantly favorable prognostic indicator in small adenocarcinomas 2 cm or less. In contrast, patients with more aggressive disease often have tumors with little or no LG components, exhibiting predominantly compressive or destructive extension within the alveolar structure [2–4].

The newly proposed International Association for the Study of Lung Cancer/American Thoracic Society/European Respiratory Society classification system suggests that, the term BAC is no longer used and the growth pattern of BAC is referred to as LG pattern, tumors should be subclassified as adenocarcinoma in situ (AIS), minimally invasive adenocarcinoma (MIA), and invasive

Abbreviations: NSCLC, non-small cell lung cancer; p-stage, pathological stage; LG, lepidic growth; BAC, bronshioloalveolar carcinoma; AIS, adenocarcinoma in situ; MIA, minimally invasive adenocarcinoma; VVG, Victoria van Gieson; TNM, tumor; node, metastasis; HE, hematoxylin and eosin; OS, overall survival; RFS, recurrence-free survival; EGFR, epidermal growth factor receptor.

* Corresponding author at: Pathology Division, Research Center for Innovative Oncology, National Cancer Center Hospital East, 6-5-1, Kashiwanoha, Kashiwa-City, Chiba 277-8577, Japan. Tel.: +81 0 4 7134 6855; fax: +81 0 4 7134 6865.
E-mail address: gishii@east.ncc.go.jp (G. Ishii).

0169-5002/$ – see front matter © 2012 Elsevier Ireland Ltd. All rights reserved.
http://dx.doi.org/10.1016/j.lungcan.2012.10.013

adenocarcinoma [5]. It was also suggested that invasive adenocarcinomas are classified according to predominant subtype. Of special interest is the new categories AIS and MIA that represent small (≤3 cm), solitary adenocarcinomas consisting purely of LG component lacking invasion or predominantly of LG component with ≤0.5 cm of invasion, repspectively. However, LG predominant larger adenocarcinoma (>3 cm) with minimally invasion was not defined in this classification.

Several researchers have similarly reported that a proportion of LG components was associated with tumor aggressiveness and prognosis in small adenocarcinomas 3 cm or less in size [6]. However, to our knowledge, there have been no reports which have described LG components in adenocarcinomas greater than 3 cm in size, and the clinicopathological significance of LG components of these tumors remains unclear.

With these backgrounds, we aimed to explore the clinical behavior and histopathological characteristics of LG predominant node-negative adenocarcinomas 3–5 cm in size because it will facilitate to clarify the association between tumor size and non-invasive properties. And it may provide new insight about progression pattern of adenocarcinoma additionally.

2. Patients and methods

2.1. Patients

During the period from January 2000 to December 2005, a total of 1428 patients underwent surgical resection for primary lung cancer at our institution, and there were 947 patients with pathologically diagnosed adenocarcinoma. Of these, 135 consecutive patients with adenocarcinoma of the lung who had undergone complete resection of adenocarcinoma 3–5 cm in size without pathological lymph node involvement were the subject of this study. There were 72 men (53.3%) and 63 (46.7%) women, with a median age of 68 years (range: 20–86 years).

All patients had a solitary lesion, and patients who had received chemotherapy or thoracic radiation before or after surgery, who underwent limited resection less than lobectomy, or who did not undergo systematic lymph node dissection were excluded. The preoperative evaluation included a physical examination, blood chemistry analysis, measurement of tumor markers, bronchofiberscopy, chest radiography, and computed tomography (CT) of the chest.

On the basis of our postoperative follow-up policy, we examined patients at 3-month intervals for the first 2 years and typically at 6-month intervals thereafter, on an outpatient basis, and aimed at continuing follow-up for 10 years after resection. The follow-up evaluation included physical examination, chest radiography, and blood examination, including pertinent tumor markers. Whenever any symptoms or signs of recurrence were detected, further evaluation were performed, including CT of the chest and abdomen, brain MRI, bone scintigraphy. Since 2004, integrated PET scan and CT scan has also been performed when appropriate.

Data collection and analyses were approved, and the need to obtain written informed consent from each patient was waived by the Institutional Review Board in February 2011.

2.2. Histopathologic analysis

Surgically resected specimens from every case were fixed with 10% formalin or pure methyl alcohol and embedded in paraffin. Tumors were cut into 5-mm slices, and serial 4-μm sections were stained with hematoxylin and eosin (HE), alcian blue periodic acid Schiff stain, and Victoria blue-Van Gieson (VVG). All slides containing the maximum surface area of the tumor from each case were coded and masked for identifiable information, and were reviewed by 2 pathologists (Y.T. and G.I.). The median of slides from each case we reviewed in our study was 9 (range: 5–21).

Histological type was determined according to the World Health Organization classification [1], and disease stages were based on the TNM classification of the Union for International Control of Cancer, 7th edition [7,8]. The histological patterns were divided into distinct subtypes, and we assessed the proportion of each component: BAC/LG, acinar adenocarcinoma, papillary adenocarcinoma, and solid adenocarcinoma with mucin production. The presence of each component was recorded as the percentage of the total tumor composition in 10% increments. An LG component was considered to be positive if the tumor cells showed pure lepidic growth without invasive lesions (Fig. 1A–C) [1]. We performed univariate prognostic analysis employing various percentage cut-offs of LG components in 10% increments, to obtain the cut-off percentage that yielded the most evident difference in prognosis when the groups above and below the cut-off were compared.

2.3. Variables for prognostic analysis

We reviewed the medical records of each patient for their clinical data. The following 8 clinicopathological factors were assessed in the prognostic analysis: age (<68 years vs. ≥68 years), gender, smoking history (<20 pack-years vs. ≥20 pack-years), preoperative serum carcinoembryonic antigen level (CEA, institutional normal cut-off level: 5.0 ng/mL, <5.0 ng/mL vs. ≥5.0 ng/mL), pleural invasion (absence vs. presence), vascular invasion (absence vs. presence), lymphatic permeation (absence vs. presence), and percentage of LG components.

2.4. Measurement of non-cancerous cell collapse area

Fig. 1 shows the representative histological findings of a case with predominant LG components (80%), seen mostly in the tumor periphery (Fig. 1B and C). In the center of such tumors, a relatively large collapse area with few or no cancer cells was often observed (Fig. 1D). We defined these areas without cancer cells, which areas were separated from the closest cancer cells by greater than 1 mm, as non-cancerous cell collapse areas (NCCA). We identified collapse area on VVG staining (Fig. 1F) and then marked NCCA according to the definition on each maximum tumor surface area slide under a microscope and captured digital photographic images on a 20× magnification field (Fig. 1A and E dot-line). These images were then traced and measured for their marked areas by using an image analysis software, Image J (NIH, Bethesda, MD). NCCA was represented as percentage of maximum tumor surface area.

2.5. Measurement of tumor disappearance rate on chest computed tomography

To investigate the correlation between the proportion of LG component and computed tomographic findings, we compared tumor disappearance rate (TDR) in the histologically most representative 20 cases each from the 2 groups: LG-dominant type (LG component occupying 50% or more of the entire tumor) and non-LG dominant type. We calculated TDR using the following definition of tumor dimensions on chest high-resolution CT [9]: pDmax, the maximum dimension of a tumor on pulmonary window setting images; pDperp, the largest dimension perpendicular to the maximum axis on pulmonary window setting images; mDmax, the maximum dimension of a tumor on mediastinal window setting images; mDperp, the largest dimension perpendicular to the